iScience

CellPress
OPEN ACCESS

Article

Secretory mouse quiescin sulfhydryl oxidase 1 aggregates defected human and mouse spermatozoa in vitro and in vivo

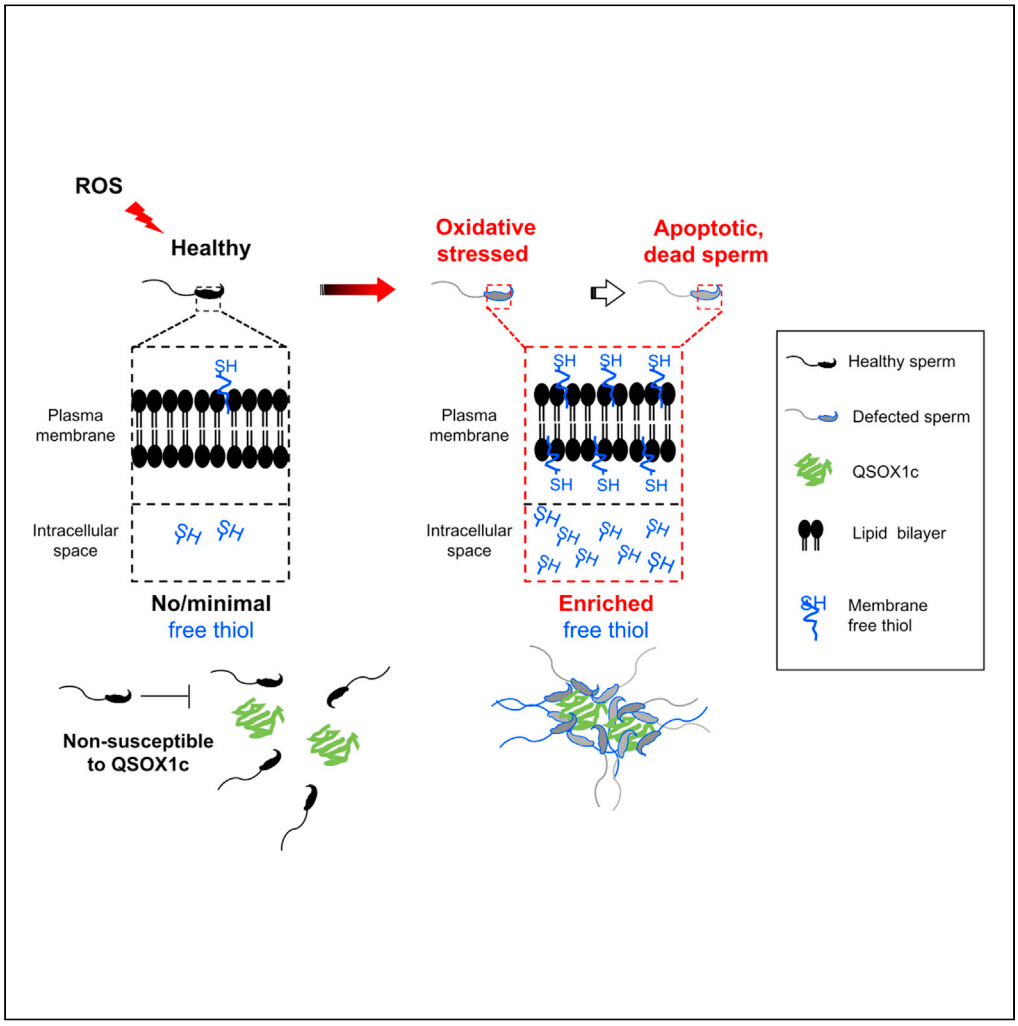

Tse-En Wang, Ling-Yu Yeh, Robert Kuo-Kuang Lee, ..., Radhika Joshi, Pei-Shiue Tsai, Sheng-Hsiang Li

psjasontsai@ntu.edu.tw (P.-S.T.)
lsh@mmh.org.tw (S.-H.L.)

Highlights

QSOX1c is expressed in the seminal vesicle and presented in the seminal plasma

QSOX1c agglutinates thiol-rich, oxidatively stressed, and apoptotic sperm

QSOX1c aggregates impaired sperm presented in the mouse uterine and human ejaculates

QSOX1c-treated semen may improve the sperm quality for artificial insemination

Wang et al., iScience 24, 103167
October 22, 2021
https://doi.org/10.1016/j.isci.2021.103167

iScience

CellPress
OPEN ACCESS

Article

Secretory mouse quiescin sulfhydryl oxidase 1 aggregates defected human and mouse spermatozoa in vitro and in vivo

Tse-En Wang,[1,2,3,9] Ling-Yu Yeh,[4,9] Robert Kuo-Kuang Lee,[4,5] Chung-Hao Lu,[5] Tsung-Hsien Yang,[4] Yu-Wen Kuo,[1,2,6] Radhika Joshi,[2] Pei-Shiue Tsai,[1,2,7,*] and Sheng-Hsiang Li[4,8,10,*]

SUMMARY

A flavin-dependent enzyme quiescin Q6 sulfhydryl oxidase 1 (QSOX1) catalyzes the oxidation of thiol groups into disulfide bonds. QSOX1 is prominently expressed in the seminal plasma. However, its role in male reproduction is elusive. Here, we purified the secreted form of QSOX1, i.e., QSOX1c, from mouse seminal vesicle secretions and revealed for the first time its function involved in sperm physiology. Exogenous addition of QSOX1c time-dependently promoted the in vitro aggregation of thiol-rich, oxidative stressed, and apoptotic mouse and human sperm cells. Also, in vivo aggregated sperm cells collected from mouse uterine and human ejaculates also showed high levels of QSOX1c, intracellular reactive oxygen species, annexin V, and free thiols. In summary, our studies demonstrated that QSOX1c could agglutinate spermatozoa susceptible to free radical attack and apoptosis. This characteristic may provide an opportunity to separate defective sperm cells and improve sperm quality before artificial insemination in humans and animals.

INTRODUCTION

The formation of gametes involves many events; these stage-wise and highly regulated processes ensure gametes undergo necessary post-spermatogenesis or post-oogenesis modifications to acquire full competence for successful fertilization. For sperm cells, morphological developments occur in the testis upon spermatogenesis; however, spermatozoa undergo continuous maturational changes in the epididymis, where they are rendered with motility and fertilization potential (Gadella, 2017; Kuo et al., 2016). Additional post-spermiogenesis alterations, including activation or inactivation of sperm activity by seminal vesicle contents at the time of ejaculation, mark the completion of spermatogenic development. Proteins secreted from the epididymis and the seminal vesicle play a pivotal role in sperm surface modifications and maturation as maturing spermatozoa are transcriptional and translational inactive with minimal and packed cytosol (Gadella, 2017; Kuo et al., 2016).

Quiescin Q6 sulfhydryl oxidase 1 (QSOX1) belongs to a protein family named quiescin Q6-sulfhydryl oxidases (QSOX) that was first discovered in the rat seminal vesicle (Ostrowski et al., 1979a). This family of oxidoreductases is dependent on flavin adenine dinucleotides (FADs) for their activity and is primarily involved in the catalysis of sulfhydryls (also called thiols) to disulfide bonds (Chakravarthi et al., 2007). Owing to its catalytic activity, QSOX1 has been implicated in protein folding, extracellular matrix elaboration, endoplasmic reticulum homeostasis, and cell cycle regulation (Kodali and Thorpe, 2010). Moreover, protective roles of QSOX1 have also been characterized; for example, QSOX1 provides myocardial cell protection against acute stress-induced apoptosis in mice (Caillard et al., 2018). Recently, evidence from independent groups demonstrated the importance of QSOX1 in cancer biology as overexpression of QSOX1 was observed in multiple malignant tumors, suggesting its participation in tumor cell invasion and metastasis (Fifield et al., 2020; Knutsvik et al., 2016; Sung et al., 2018). Although QSOX1 has created its niche in cancer biology, including its potentials as a prognostic marker for cancer detection (Lake and Faigel, 2014), the role of QSOX in reproductive biology, or sperm physiology is understudied and remains elusive.

QSOX1 is ubiquitously distributed in the male reproductive system, such as testis, epididymis, vas deferens, and seminal vesicle (Portes et al., 2008; Tury et al., 2006; Wang et al., 2018). We previously showed

[1]Department of Veterinary Medicine, National Taiwan University, Taipei, Taiwan

[2]Graduate Institute of Veterinary Medicine, National Taiwan University, Taipei, Taiwan

[3]Department of Cellular and Molecular Physiology, Yale School of Medicine, New Haven, USA

[4]Department of Medical Research, MacKay Memorial Hospital, Tamsui, Taiwan

[5]Department of Obstetrics and Gynecology, MacKay Memorial Hospital, Taipei, Taiwan

[6]Department of Clinical Sciences, Swedish University of Agricultural Sciences, Uppsala, Sweden

[7]Research Center for Developmental Biology and Regenerative Medicine, National Taiwan University, Taipei, Taiwan

[8]MacKay Junior College of Medicine, Nursing, and Management, Taipei, Taiwan

[9]These authors contributed equally

[10]Lead contact

*Correspondence: psjasontsai@ntu.edu.tw (P.-S.T.), lsh@mmh.org.tw (S.-H.L.)

https://doi.org/10.1016/j.isci.2021.103167

that QSOX1 and 2 exhibited complementary epididymal distribution and possessed distinct subcellular localizations within the epididymal principal cells. Moreover, distinct associations of QSOX1 variant c (QSOX1c, the secretory form of QSOX1) and QSOX2 with sperm acrosome and implantation fossa were observed, suggesting QSOX1c and QSOX2 have discrete biological functions in male germ cell development (Wang et al., 2018). In this study, we aim to unravel the functional involvement of QSOX1c in the male reproductive system, specifically, its roles and interactions with post-spermiogenesis sperm cells.

RESULTS

QSOX1c purification, characterization, antibody specificity, and tissue distribution assessments

Mouse seminal vesicle secretion (SVS) was fractionated by anion-exchange chromatography on a diethylaminoethyl (DEAE)-Sephacel column and ion-exchange high-performance liquid chromatography (HPLC) on a sulfopropyl column (Figures S1A and 1B). The peak e protein of the HPLC sulfopropyl column (Figure S1B) was yellow-colored, which is consistent with the characteristics of QSOX1 with the yellow cofactor FAD (Ostrowski et al., 1979b). When SDS-PAGE reducing gel was subsequently performed, a relative homogenous band of approximately 65-kDa was observed (Figure S1C, indicated with red arrowhead). To resolve the 65-kDa protein identity, we excised the band, digested it with trypsin, and determined each tryptic peptide molecular mass using MALDI-TOF mass spectral analysis. The tryptic peptide sequences identified from the spectral peaks a-e (Figure S1D) were LNDIDGFFTR (residues 176-185), EFNIAGFPTVR (residues 115-125), SYVQFFFGCR (residues 444-453), NGSGATLPGAGANVQTLR (residues 133-150), and YSEAHPQEPADGQEVLQAMR (residues 424-443), respectively (Figure S1E). Based on the theoretical mass determined for each peptide fragment, the peak e sample identified in Figure S1C ("Pe" under HPLC) was predicted to be the protein sequence deduced from the precursor of quiescin Q6 sulfhydryl oxidase 1 (NCBI reference sequence: NP_075757.1). The N-terminal amino acid sequence determined using automated Edman degradation for the 65-kDa protein was assembled to ARLSVLYSSSDPLTLLDAD, matching with the predicted N-terminal sequence of the precursor protein (Figure S1E). QSOX1 has four isoforms produced by alternative splicing with UniProt identifiers Q8BND5-1∼4 (https://www.uniprot.org/uniprot/Q8BND5). The HPLC-purified 65-kDa protein could be the isoform 3 according to its molecular weight; we named it as mouse QSOX1c.

When protein components from SVS and fractions of each purification samples shown in Figure S1C were immunoblotted with antiserum against QSOX1c, specific protein bands corresponding to the 65-kDa (indicated with red arrowhead, Figure S1F) can be recognized among hundreds of mouse SVS proteins, fraction 3 of DEAE-Sephacel chromatography, and peak e of HPLC, indicated the high specificity of the antiserum against QSOX1c was generated (compare Figures S1C and S1F).

We next examined tissue distribution of QSOX1c in mouse reproductive tissues. As shown in Figure 1A, the seminal vesicle (S) expressed the most abundant QSOX1c. In line with our previous studies, male reproductive tissues, such as testis, epididymis, vas deferens, copulating gland, and prostate also expressed QSOX1c (Kuo et al., 2017; Wang et al., 2018); however, when compared with male, female reproductive organs examined (i.e., ovary, oviduct, and uterus) showed relatively low protein expression of QSOX1c. In addition to the 65-kDa band, the antiserum against QSOX1c may also recognize other QSOX1 isoforms in the testis and seminal vesicle but awaits further investigation. Furthermore, the antiserum also specifically recognized the ∼65-kDa secreted QSOX1 from thousands of human seminal plasma proteins (Figure S2).

To quantify the physiological concentration of QSOX1c in SVS, various amounts of purified QSOX1c and the SVS were resolved in an SDS-PAGE gel and analyzed using Western blotting and ImageJ software. Based on quantitative analysis, the physiological concentration of QSOX1c in SVS was estimated to be approximately 0.1–0.6 mg/mL.

Testosterone upregulated *Qsox1* mRNA and QSOX1c protein expression levels

Sex hormones mostly regulate protein expression in reproductive organs; among all known male androgen, testosterone is one of the dominant sex hormones (Dohle et al., 2003; Robaire and Hamzeh, 2011; Turner et al., 1985); therefore, we next investigated whether testosterone regulates mouse *Qsox1c* expressions (both mRNA and protein) in the male reproductive tissue. Northern blotting analysis showed that when compared with testes-removal (castrated, corn oil) animals, testosterone upregulated *Qsox1*

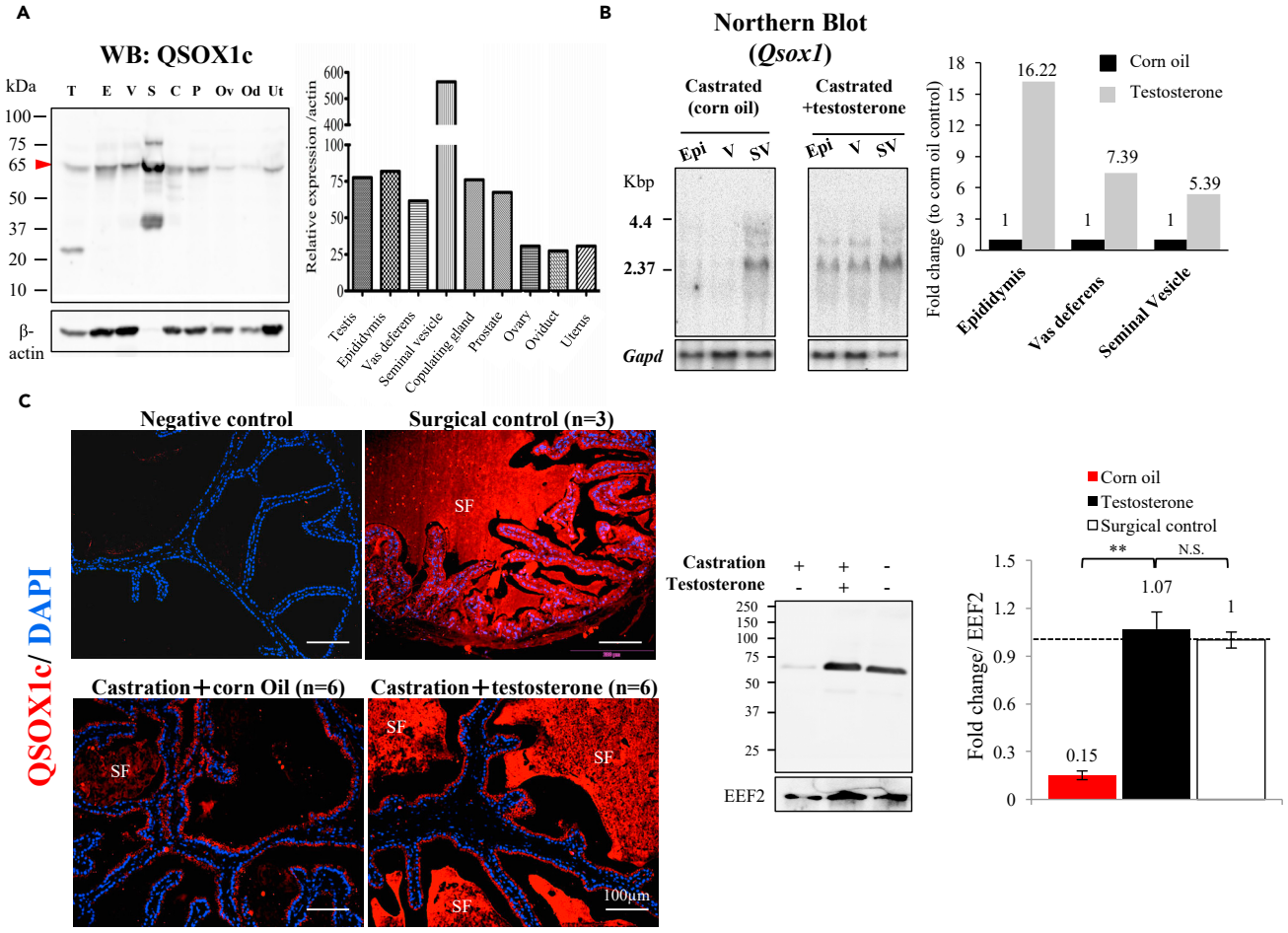

Figure 1. Testosterone up-regulated QSOX1c expression in male reproductive organs

(A) Tissue distribution analysis showed that QSOX1c was enriched in male reproductive organs. SVS: seminal vesicle secretion; f1-4: fraction 1-4; Pa-e: peak a-e; T: testis; E: epididymis; V: vas deferens; S: seminal vesicle; C: coagulating gland; P: prostate; Ov: ovary; Od: oviduct; Ut: uterus.

(B) Northern blot analysis showed that QSOX1 RNA expression was down-regulated after castration. Testosterone administration increased the expression of QSOX1 RNA in the epididymis, vas deferens, and seminal vesicle by 16.22-, 7.39-, and 5.39-fold, respectively.

(C) Indirect immunostaining and western blot analysis of seminal vesicle samples also supported the evidence that testosterone up-regulated the protein expression of QSOX1c. Epi: epididymis; V: vas deferens; SV: seminal vesicle; SF: seminal vesicle fluid. N.S.: not significant; **: $p < 0.01$, Representative images from 6 individual animals were presented.

mRNA expression in the epididymis (16.22-fold), vas deferens (7.39-fold), and seminal vesicles (5.39-fold) (Figure 1B). In line with mRNA expression, protein levels of mouse QSOX1c in the seminal vesicles were downregulated in castrated mice as only weak signals were detected along the epithelium of the seminal vesicle (Figure 1C). In contrast, testosterone administration significantly rescued the castration-induced downregulation of QSOX1c in mouse seminal vesicles (Figure 1C). These findings suggest that *Qsox1* is regulated by testosterone.

QSOX1c inhibited sperm capacitation, acrosome reaction and aggregated both mouse and human sperm in vitro

To elucidate the functional involvement of QSOX1c in sperm physiology, we incubated mouse epididymal sperm with purified mouse QSOX1c. As shown in Figure 2A, BSA remarkably induced sperm protein tyrosine phosphorylation compared to the control medium alone (see lanes 1 and 2). Addition of QSOX1c alone did not alter sperm protein tyrosine phosphorylation (Figure 2A, lane 6) as the level of sperm protein tyrosine phosphorylation was similar to that of the control group (compared lane 1 and 6). Unexpectedly, QSOX1c did inhibit BSA-induced phosphorylation levels; however, the reduced phosphorylation levels did not show a dose-dependent manner (Figure 2A, lane 3–5).

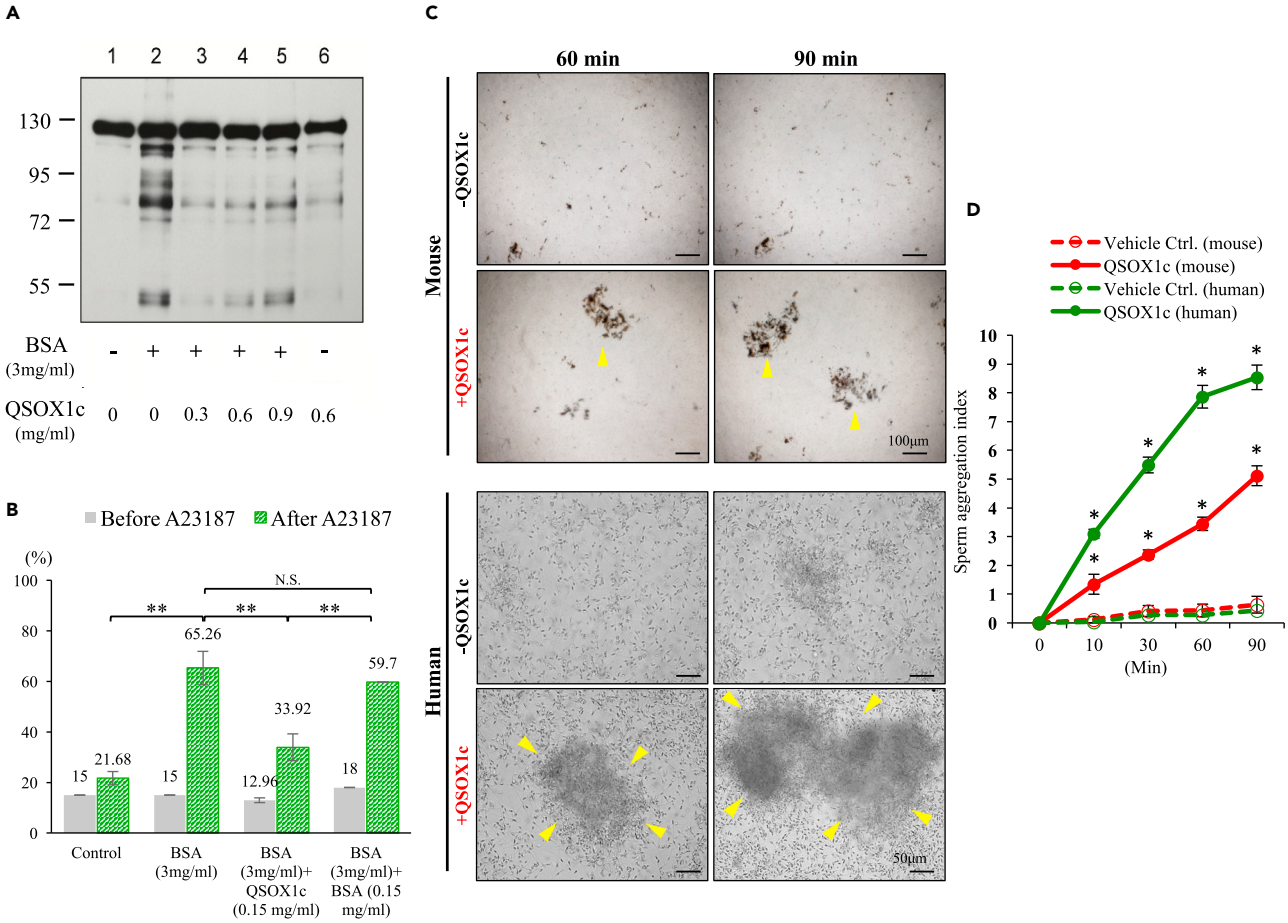

Figure 2. QSOX1c inhibited sperm capacitation, acrosome reaction and induced in vitro sperm agglutination in humans and mice

(A) The effect of QSOX1c on sperm capacitation capacity reflected from the level of sperm protein tyrosine phosphorylation. In contrast to 3 mg/mL BSA induced a significant level of sperm protein tyrosine phosphorylation, when mouse sperm cells were co-incubated with 0.3-0.9 mg/mL purified QSOX1c, the tyrosine phosphorylation level was significantly reduced.

(B) The effect of QSOX1c on sperm acrosome reaction. Epididymal spermatozoa were capacitated in the presence of BSA and/or QSOX1c at 37°C for 90 min. Sperm acrosome reaction induced by calcium ionophore A23187 (right green column) or un-induced (left gray column) was evaluated by PNA staining. Con, medium only, negative control; BSA, positive control for sperm capacitation; BSA + QSOX1c and BSA + BSA (0.15 mg/mL), the experimental groups to evaluate the influence of QSOX1c. As shown on the left gray columns, sperm acrosome was intact after incubation at different conditions; however, the majority of the sperm acrosome was lost after A23187 ionophore treatment at the BSA and BSA + BSA (0.15 mg/mL) groups. Intriguingly, the agglutinated sperm were not able to undergo acrosome reaction in the presence of QSOX1c.

(C) Sperm aggregates (indicated with arrowheads) can be observed when sperm cells were added into the incubation media. However, a significant time-dependent increase in the number and size of sperm aggregates was observed in vitro when mouse or human sperm cells were incubated with 0.15 mg/mL purified mouse QSOX1c.

(D) Quantitative analysis demonstrated the increase of sperm aggregation in both mouse and human sperm in vitro. Comparisons were carried out between with and without QSOX1c at each time point of observation (i.e., green solid line vs. green dashed line for comparisons in the human sample; red solid line vs. red dashed line for comparisons in mouse sample). Data from at least 3 independent experiments were pooled for statistical analysis. Representative images were presented. *: $p < 0.05$, **: $p < 0.01$.

When sperm acrosome status was evaluated, most of the sperm acrosome remained intact despite their presence within or outside the sperm aggregates (Figures 2B, gray bars, S3A–S3D). However, after A23187 ionophore treatment, sperm acrosome, especially in free sperm, almost disappeared (Figures S3F and S3G). Interestingly, in the presence of QSOX1c, ionophore-induced acrosome reaction was partially inhibited (Figure 2B, green bars, from 65.3% to 33.9%), and the acrosomes of agglutinated sperm remained mostly intact (Figures S3G and S3H), and this inhibitory effect was QSOX1c-specific phenomenon as the addition of the same amount of other protein (i.e., BSA) did not exert similar inhibitory effect (from 65.3% to 59.7%, Figure 2B).

When we conducted a time course experiment, although we observed a gradual increase in spontaneous sperm aggregation over time, a time-dependent increase in sperm aggregation in both mouse and human sperm cells was more pronounced in the presence of mouse QSOX1c (Figure 2C, sperm aggregations were indicated with arrowheads); to quantify QSOX1c-induced sperm aggregation, a self-defined "sperm aggregation index" was used (defined in the material and methods section and illustrated in Figure S4A). As shown in Figure 2D, in the presence of mouse QSOX1c, the time-dependent increase in sperm aggregation index was calculated in the human (green solid line) and mouse (red solid line) compared with the control group without QSOX1c. These findings suggest that the earlier observed sperm aggregation in vitro is at least, if not all, partially due to the effect of QSOX1c on sperm cells.

Mouse QSOX1c induced in vitro aggregation of oxidatively stressed mouse and human sperm cells with abundant surface free thiols

To investigate the characteristics of QSOX1c-aggregated sperm cells, a series of in vitro analyses were performed on the oxidative status of sperm, surface free thiols, and sperm viability. To assess sperm intracellular ROS and oxidative stress, a commercially available CellROX kit was used. We first tested whether the addition of mouse QSOX1c would cause changes in the basic sperm oxidative status, which may lead to evaluation bias. As shown in Figure S5A, when MitoTracker Red CM-H2XRos was used to examine sperm oxidative status, there was no significant difference between the groups with or without QSOX1c; moreover, when sperm cells were lysed for total antioxidant capacity analysis, no difference could be measured (Figure S5B). These data indicate that the addition of mouse QSOX1c does not alter the intrinsic oxidative status of sperm.

Although aggregations were observed in the control group, CellROX positive sperm cells exhibiting oxidative stress were randomly distributed in the control group (Figures 3A and 3C, -QSOX1c, only 36-39% CellROX positive was detected within the aggregated sperm). In sharp contrast, in the presence of QSOX1c, most oxidatively stressed sperm cells were detected in the aggregates (90.6% and 85.4% in mouse and human sperm, respectively) (Figures 3A and 3C) indicated that QSOX1c can aggregate oxidatively stressed sperm cells in vitro.

QSOX protein is known to catalyze free thiols to form stable disulfide bonds (Chakravarthi et al., 2007); we, therefore, examined the presence of surface and intracellular free thiols on these aggregated sperm. We observed similar results when mBBr was used to detect free thiols of mouse epididymal sperm or ejaculated human sperm. In the CellROX experiment, aggregated sperm cells showed abundant free thiols (positive for mBBr in blue) in the presence of QSOX1c. In contrast, in the absence of QSOX1c, sperm cells also contained surface free thiols but were randomly distributed within and outside sperm aggregates (Figures 3B and 3C).

QSOX1c aggregated apoptotic mouse and human sperm in vitro

Oxidatively stressed sperm cells are likely prone to apoptosis (annexin V as marker) or death (PI as marker) (Takeshima et al., 2021). We next applied the LIVE/DEAD staining kit combined with annexin V to evaluate the viability and cellular apoptosis on incubated sperm samples. As shown in Figure 4, most of the annexin V-positive sperm (86.7% and 89.8% in mouse and human sperm, respectively) were detected in the aggregates (Figures 4A–4D), indicated that mouse QSOX1c could aggregate apoptotic mouse and human sperm in vitro. Compared with annexin V, QSOX1c has no specificity on aggregating or distinguishing live or motile sperm as around 50% of the SYBR14 positive (46.2 $\pm$ 18%, 48.3 $\pm$ 15% for mouse and human sperm, respectively) and PI-positive (61.2 $\pm$ 13%, 61.3 $\pm$ 20% for mouse and human sperm, respectively) sperm cells were observed within the aggregates (Figures 4C and 4D).

Sperm aggregates in vivo showed high levels of QSOX1c, annexin V, ROS, and surface free thiols

To examine whether the sperm agglutinated by QSOX1c in vitro also occurs in vivo and whether the sperm cells aggregated in vivo share similar properties as those we observed in in vitro experiments, we obtained the ejaculated sperm from the mouse uterus and human semen for further analyses. As shown in Figure 5, sperm agglutination (indicated with arrowheads) was detected in the ejaculated sperm isolated from both mouse uterus (Figure 5A) and human semen (Figure 5B). When uterine sperm agglutinates and human semen sperm aggregates were stained for the presence of QSOX1c, evident signals were detected in all sperm aggregates (Figure 5, indicated with yellow arrowheads). Moreover, when these aggregates were

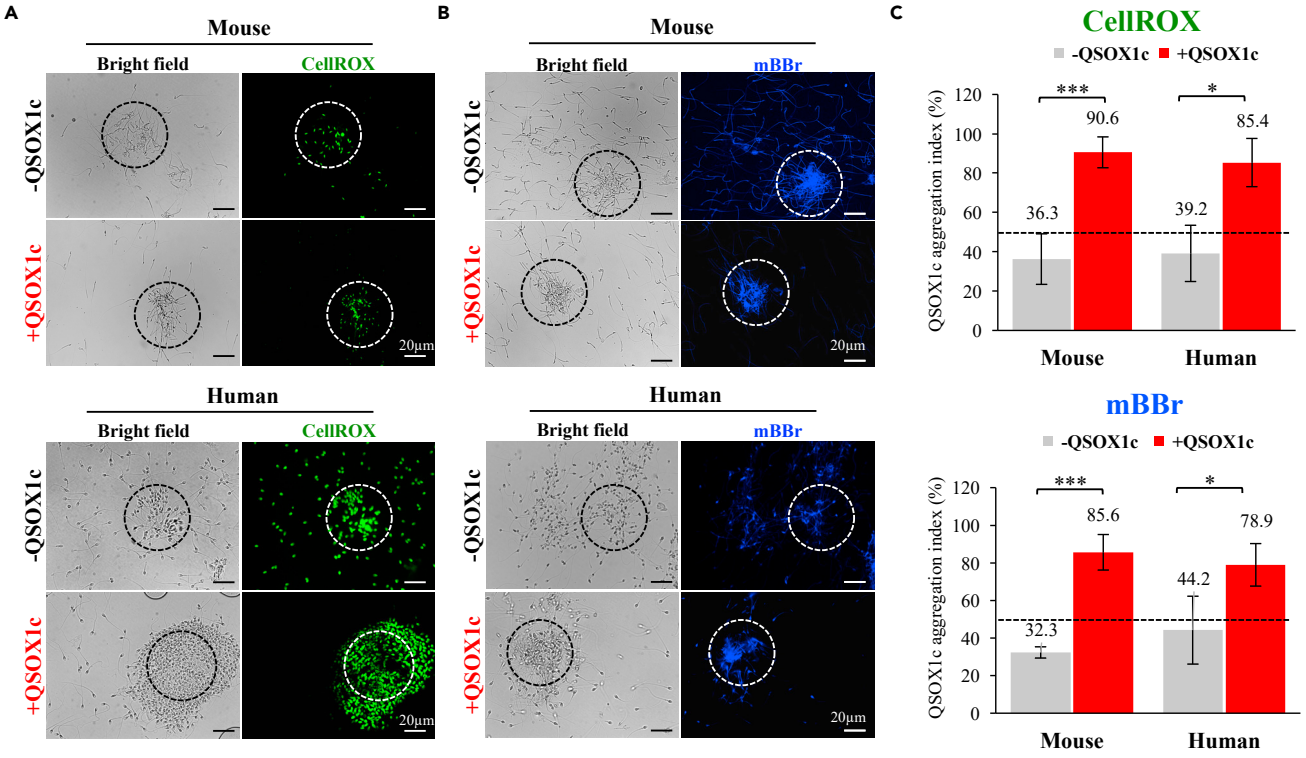

Figure 3. QSOX1c aggregated sperm were oxidatively stressed and had abundant surface free thiols

(A) When compared with scattered CellROX weak signals among the observed areas in the control group, in the presence of purified mouse QSOX1c, most of the CellROX positive sperm cells were only detected in the aggregates.

(B) When mBBr was used to detect sperm free thiol, sperm cells showed positive signals at different regions of the sperm surface. In the presence of purified mouse QSOX1c, most mBBr positive sperm cells were detected in the aggregates. Sperm aggregations measured were circled.

(C) Quantitative analysis showed most of CellROX-positive and mBBr-positive mouse and human sperm cells were being aggregated after the addition of QSOX1c protein. The dashed line indicated that a 50% threshold is used to distinguish between random inclusions of sperm into the aggregates or the inclusion of sperm cells in the aggregates being a QSOX1c-related event. More than 50% suggests a QSOX1c-specific consequence caused by the addition of QSOX1c. Data from at least 3 independent experiments were pooled for statistical analysis. Representative images were presented. *: $p < 0.05$, ***: $p < 0.001$. Dash line indicated 50%.

further examined for specific markers, in line with our in vitro data, we observed a high level of annexin V positive (77.9%, 82% for mouse and human sperm, respectively), CellROX positive (81.3%, 79.3% for mouse and human sperm, respectively), and mBBr positive (92.7%, 90% for mouse and human sperm, respectively) sperm cells in the aggregations and only minor scatter signals can be detected outside the sperm aggregation (Figure 6). These data not only validated our in vitro observations but also supported that QSOX1c can aggregate defected sperm cells across species (at least in mice and humans) in vitro and in vivo.

DISCUSSION

Since Qstrowski et al. first discovered sulfhydryl oxidase from rat SVS (Ostrowski et al., 1979b), most of the studies regarding the function of QSOX protein focused on its biochemical activity (Ostrowski et al., 1979b; Ostrowski and Kistler, 1980; Rudolf et al., 2013) and its relation with breast, pancreas, and prostate cancers (Lake and Faigel, 2014; Sobral et al., 2015; Sung et al., 2018). However, up to date, besides tissue or cellular distributions of QSOX proteins, no information is available on the functional involvement of QSOX proteins in reproduction. In this study, we demonstrated for the first time that purified QSOX1c protein from mouse SVS can aggregate defected mouse and human sperm both in vitro and in vivo; more importantly, QSOX1c-aggregated sperm cells exhibited a high level of intracellular ROS, surface/intracellular free thiol, apoptotic marker protein annexin V and dead sperm marker PI. These specific properties suggested that QSOX1c exhibited potentials to aggregate defected sperm cells and may serve as a selection material to enable the removal of defected sperm and to improve semen/sperm quality before artificial insemination in both human and animals.

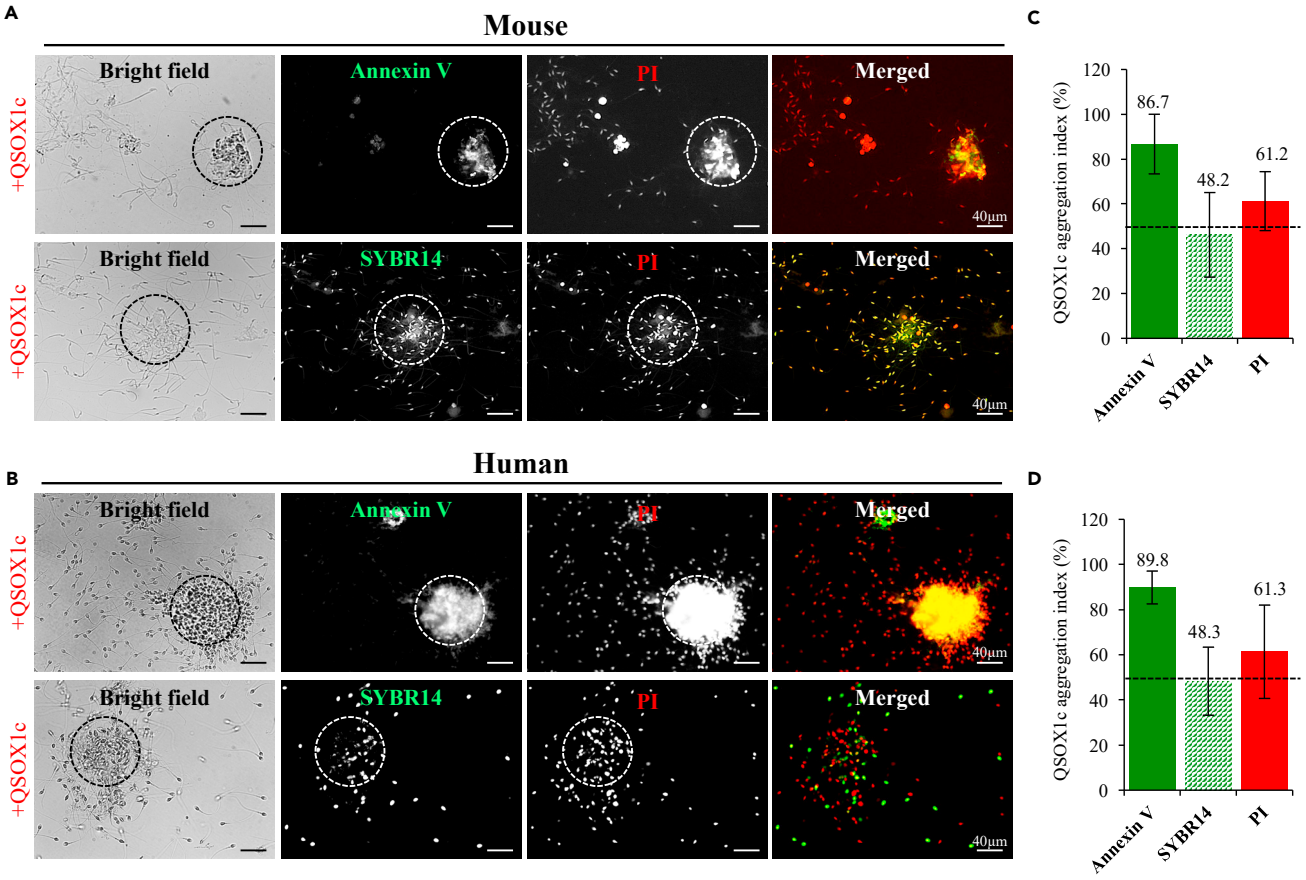

Figure 4. QSOX1c aggregates apoptotic, but not immotile or dead human and mouse sperm in vitro

(A and B) When purified QSOX1c was added into the incubation media, we observed the aggregated sperm cells for both mouse (A) and human (B) sperm were mostly positive for apoptosis marker, annexin V staining; in contrast to annexin V, the addition of mouse QSOX1c did not lead to aggregation of dead sperm (indicated by propidium iodide, PI) cells.

(C and D) Quantitative analysis showed most of the annexin V positive mouse (86.7%) and human (89.8%) sperm cells were being aggregated after the addition of QSOX1c protein. In contrast, only 48% of SYBR14 positive and 61% of PI-positive sperm cells were being aggregated. Sperm aggregations measured were circled. The dashed line indicated a 50% threshold was used to distinguish between random inclusions of sperm into the aggregation or the inclusion of sperm cells in the aggregates was a QSOX1c-related event. More than 50% suggested a QOSX1c-specific consequence caused by the addition of QSOX1c. Data from 3 independent experiments were pooled for calculation of means and SD. Representative images were presented. Dash line indicated 50%.

Mature sperm cells have been shown to interact with each other by cohesive force upon transit within reproductive tracts (Fisher and Hoekstra, 2010; Monclus and Fornes, 2016). The "head-to-head" sperm conjugation is commonly observed at the distal segment of the epididymis (i.e., cauda) or inside the female genital tract (Monclus and Fornes, 2016; Suarez and Pacey, 2006); this specific and reversible phenomenon has been considered as part of the sperm maturation processes that in favor of sperm competition as conjugated sperm cells are faster in moving forward and are less prone for spontaneous acrosome reaction before reaching the oocyte (Gómez Montoto et al., 2011; Suarez, 2016; Tourmente et al., 2011). One of the important characteristics of this naturally formed "head-to-head" sperm conjugation is the dynamic assemble-disassemble changes along with their progression toward the oocyte. As the disassembling process occurs at the time of capacitation, it allows sperm to efficiently fertilize an oocyte but not leads to polyspermy fertilization (Monclus and Fornes, 2016).

Although we observed similar sperm clumps in this study; however, unlike "head-to-head" sperm conjugation, we observed that QSOX1c-induced sperm aggregates formed random binding patterns of head-to-head, head-to-tail, and tail-to-tail. Moreover, most "head-to-head" sperm conjugates are smaller in size, composed of 3–6 sperm cells (Fisher and Hoekstra, 2010; Monclus and Fornes, 2016; Taggart et al., 1993); we observed in this study

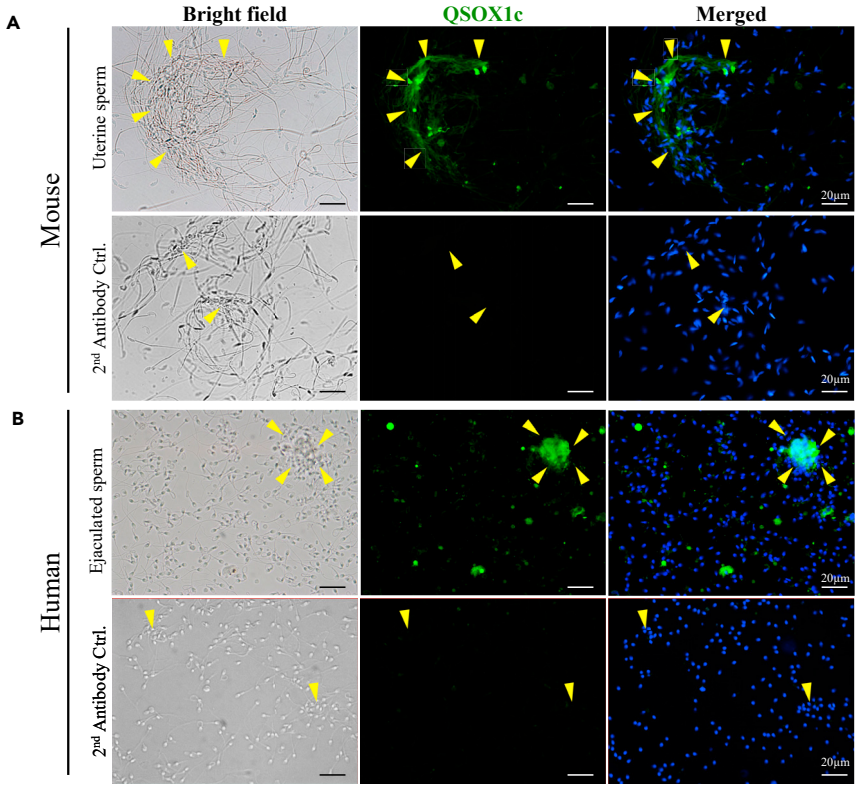

Figure 5. Mouse and human sperm aggregates were enriched with QSOX1c protein in vivo

(A) Mouse uterine sperm collected after mating showed similar sperm aggregation as observed in vitro. When sperm aggregates were stained for QSOX1c, we observed a strong QSOX1c signal present in the aggregated sperm clumps (indicated with arrowheads). This is not due to the antibody's non-specific aggregation, as no signal was detected in sperm aggregations of the 2nd antibody control group.

(B) Similar results were observed in human sperm samples collected from the liquefied semen as a strong QSOX1c signal was detected at the sperm aggregations. Data from 3 independent experiments were evaluated, and representative images were presented.

that QSOX1c-induced sperm clumps showed a time-dependent increase in number and size that sometimes composed up to 20-50 sperm cells. These above-mentioned observations clearly indicated that although QSOX1c protein is detected in both male and female reproductive tracts, QSOX1c-induced sperm aggregation is distinct from the earlier described "head-to-head" formation of sperm conjugation and likely participate in the random binding of two free thiols (inter-sperm) present on sperm membrane surface owing to QSOX1's enzyme activity on catalyzing disulfide bond formation (Grossman et al., 2013; Rudolf et al., 2013). Another evidence supporting the differences between QSOX1c-induced aggregations from "head-to-head" sperm conjugation is that unlike high proportion of motile and alive sperm cells should present in the "head-to-head" sperm conjugation, we observed QSOX1c did not tend to aggregate motile sperm as in the presence of QSOX1c protein, less than 50% of the live sperm was detected inside the aggregation. Taken together, we proposed that there are two types of naturally formed sperm conjugations; the head-to-head sperm conjugation facilitates sperm forward movement and preserves sperm acrosome to prevent immature acrosome reaction before sperm reaching the oocyte. The QSOX1c-induced random binding of sperm cells serves to aggregate defected sperm and likely facilitates recognition and clearance of bad quality sperm cells by uterine polymorphonuclear leukocytes as described by Robertson (Robertson, 2007) and Katila (Katila, 2012).

Another interesting observation is that QSOX1c is highly enriched in the seminal vesicle with relatively less expression in the female reproductive tract. QSOX1c in the SVS, together with spermatozoa, are released into semen upon ejaculation. In mice, SVS mixes with semen and directly enters the uterus (Li and Winuthayanon, 2017), while in humans, semen is deposited at the anterior wall of the vagina, next to the external orifice of the cervix (Suarez and Pacey, 2006); QSOX1c, instead of serving as a sperm conjugating factor that

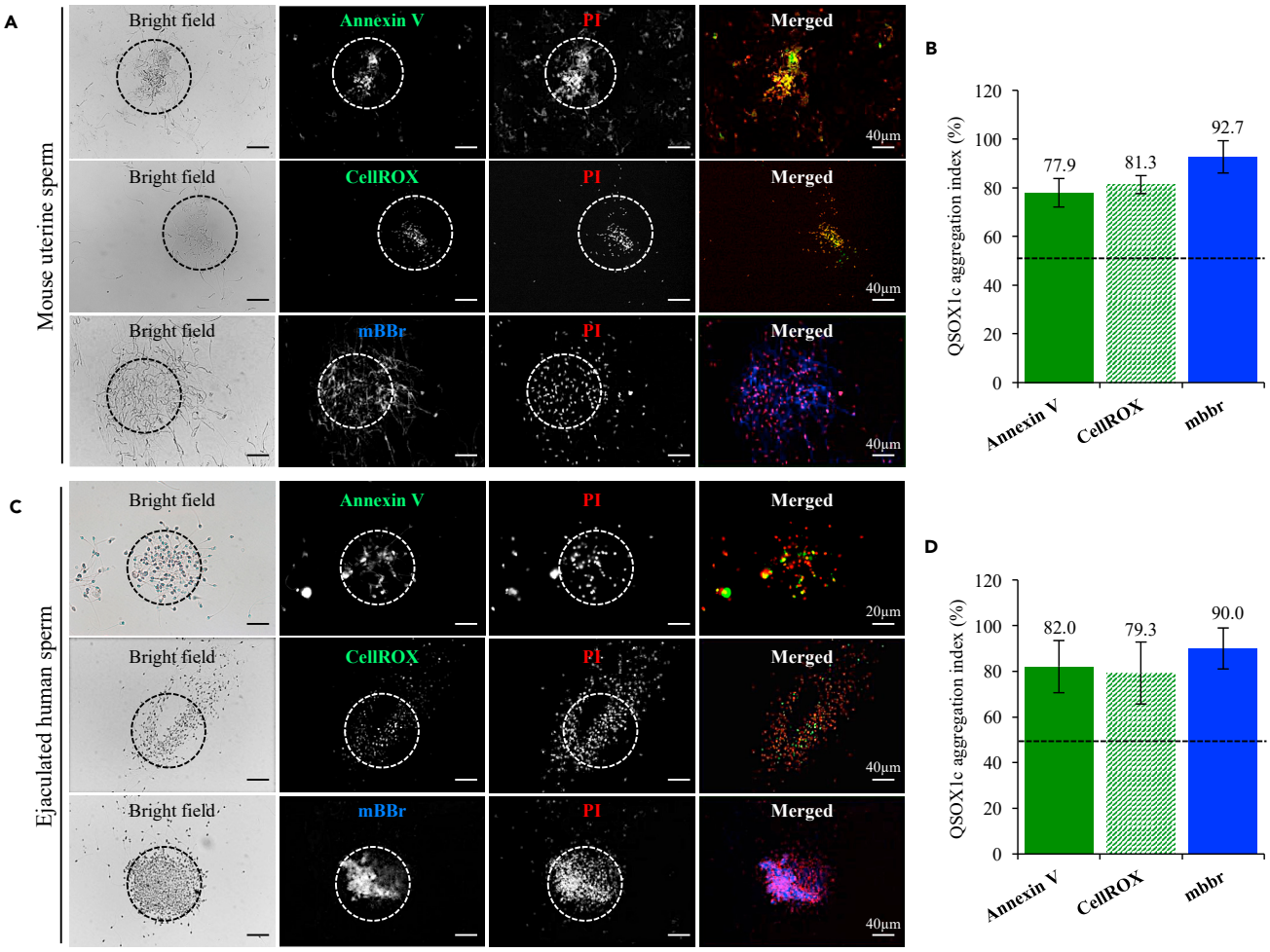

Figure 6. Aggregated mouse uterine sperm and non-processed human sperm showed high levels of annexin V, ROS, and surface free thiols

(A–D) When sperm cells of in vivo conditions (mouse uterine sperm and human non-processed human sperm) were examined for the presence of apoptotic marker, oxidative stress, and surface free thiols, we observed as in vitro findings that 78-82% of the mouse (A and B) and human (C and D) sperm cells that are positive for annexin V (solid green bar in (B and D)) were detected in the sperm aggregates. Similar results were detected for CellROX, and surface free thiols as 79-81% of the CellROX positive sperm indicated oxidatively stressed sperm cells were detected within sperm aggregates (dashed green bar in (B and D)). When mBBr was used to indicate the amount of sperm free thiol, we observed 90-92% of the sperm cells with positive signals for mBBr were aggregated into sperm clumps (blue bars in (B and D)). The dashed line indicated a 50% threshold was used to distinguish between random inclusions of sperm into the aggregation or the inclusion of sperm cells in the aggregates was a QSOX1c-related event. More than 50% suggested a QSOX1c-specific consequence caused by the addition of QSOX1c. Data from 3 independent experiments were pooled for calculation of means and SD. Representative images were presented. Dash line indicated 50%.

facilitates sperm competition in the female reproductive tract, may act to aggregate a specific population of defected sperm that eventually will be left out at the proximal part of the female reproductive tract. Our in vitro and in vivo experiments further supported this speculation that sperm cells in QSOX1c-induced aggregates showed high levels of ROS and surface and/or intracellular mBBr (indicating the presence of free thiols) and were positive for apoptosis marker annexin V. An earlier study showed flavin-linked sulfhydryl oxidases participate in the net formation of disulfide bonds in oxidized protein folding (Kodali and Thorpe, 2010). The appearance of oxidized protein on the surface of oxidatively stressed sperm cells with free sulfhydryl groups may contribute to inclined QSOX1c association.

The phenomenon of sperm conjugation has been observed in many species, such as opossum (Bedford and Yanagimachi, 1992), rodents (Cooper et al., 2000; Fornes and Burgos, 1994), and loris (Phillips and Bedford, 1987), and has been suggested to protect sperm acrosome to preserve the sperm integrity. As for this study, although QSOX1c-agglutinated sperm cells contain intact acrosomes; however, the aggregated

sperm cells showed various defected characteristics. Unlike sperm aggregates, healthy free sperm can be induced for capacitation and undergo a calcium ionophore-induced acrosome reaction; however, QSOX1c seems to inhibit such responses in free sperm. We observed that QSOX1c inhibited BSA-induced sperm protein tyrosine phosphorylation and the subsequent acrosome reaction. The possible reason is that most QSOX1c-agglutinated sperm cells were defected and cannot undergo capacitation or acrosome reactions. Several seminal proteins in SVS, e.g., SERPINE2 (Li et al., 2018; Lu et al., 2011), SPINKL (Lin et al., 2008; Tseng et al., 2013), SVLLP (Ou et al., 2021), and SVS2 (Araki et al., 2015; Kawano and Yoshida, 2007), can prevent premature capacitation and subsequent acrosome reaction and preserve sperm ability to fertilize an egg before reaching the fertilization site. Thus, although more experimental evidence is needed, we speculate that QSOX1c may not exhibit similar preservation functions as the above-mentioned SVS proteins.

With the characteristics of QSOX1c to aggregate the ROS damaged (CellROX positive), apoptotic (annexin V positive), and dead sperm (PI positive), QSOX1c might be used to remove damaged sperm. Currently, commercially available annexin V-linked magnetic beads can only eliminate apoptotic sperm. However, the beads connected to QSOX1c might be more powerful to remove damaged sperm of various kinds. It is expected that the use of QSOX1c will greatly improve sperm quality before artificial reproductive technology treatments, such as intrauterine insemination, intracellular sperm injection, or in vitro fertilization.

In conclusion, we demonstrated that mouse QSOX1c is enriched in male reproductive tissues; its expression is highly regulated by testosterone. Upon ejaculation, QSOX1c from the SVS aggregates defected sperm cells, which have high levels of ROS, surface and intracellular free thiols, and apoptotic marker protein annexin V. This ability of aggregating sperm cells that nonspecifically connects the two free thiols between the defective sperm cells may be due to QSOX's natural disulfide bond catalytic activity, thus, explains murine QSOX1c can cross species to aggregate human sperm. This characteristic may potentially separate defected sperm cells from motile and well-matured sperm, which likely to improve sperm quality before artificial insemination of humans and animals.

Limitations of the study

In this study, we found that the seminal plasma protein QSOX1c can agglutinate defective sperm. However, the damaged state of sperm in the agglomerate cannot be analyzed by flow cytometry and must be observed under a microscope using fluorescent markers. When quantitatively analyzing the ratio of defective and non-defective sperm in sperm aggregates, we use our own defined sperm aggregation index for analysis. Although it may be representative, it is still not easy to analyze all sperm aggregates. Also, the mechanism of how QSOX1c agglutinates sperm remains to be further analyzed in the future.

STAR★METHODS

Detailed methods are provided in the online version of this paper and include the following:

- KEY RESOURCES TABLE
- RESOURCE AVAILABILITY
  - Lead contact
  - Materials availability
  - Data and code availability
- EXPERIMENTAL MODEL AND SUBJECT DETAILS
  - Human semen collection
  - Mice
- METHOD DETAILS
  - Purification of mouse QSOX1c protein
  - Mass spectrometry analysis
  - Production of anti-QSOX1c antisera
  - Western blotting
  - Animal castration and hormone challenge model
  - Northern blotting
  - Immunofluorescence staining on tissue sections
  - Sperm capacitation and acrosome reaction
  - Sperm oxidative status assays

- In vitro sperm aggregation assay
- In vivo sperm aggregation assay

- QUANTIFICATION AND STATISTICAL ANALYSIS

SUPPLEMENTAL INFORMATION

Supplemental information can be found online at https://doi.org/10.1016/j.isci.2021.103167.

ACKNOWLEDGMENTS

This study was supported by grants from the Ministry of Science and Technology (Grant #104-2311-B-002-022, #105-2628-B-002-022-MY3 to PS TSAI; #107-2314-B-195-006 to SH LI), Taiwan, and Ministry of Education (Grant #108L7865, #109L7865 to PS TSAI), Taiwan. This work was also supported by MacKay Memorial Hospital (Grant # MMH 10446 and 10824 to SH LI), Taipei, Taiwan. The funding bodies had no role in the design of the study and collection, analysis, and interpretation of data and in writing the manuscript.

AUTHOR CONTRIBUTIONS

Conceptualization, T.-E.W., L.-Y.Y., R.K.-K.L., P.-S.T., and S.-H.L.; methodology, T.-E.W., L.-Y.Y., C.-H.L., T.-H.Y., and S.-H.L.; investigation, T.-E.W., L.-Y.Y., C.-H.L., T.-H.Y., Y.-W.K., and R.J.; validation, C.-H.L., T.-H.Y., and L.-Y.Y.; writing—original draft preparation, supervision, and funding acquisition, P.-S.T. and S.-H.L.

DECLARATION OF INTERESTS

The authors declare no competing interests.

Received: March 25, 2021
Revised: July 8, 2021
Accepted: September 21, 2021
Published: October 22, 2021

REFERENCES

Araki, N., Trencsényi, G., Krasznai, Z.T., Nizsalóczki, E., Sakamoto, A., Kawano, N., Miyado, K., Yoshida, K., and Yoshida, M. (2015). Seminal vesicle secretion 2 acts as a protectant of sperm sterols and prevents ectopic sperm capacitation in mice. Biol. Reprod. *92*, 8. https://doi.org/10.1095/biolreprod.114.120642.

Bedford, J.M., and Yanagimachi, R. (1992). Initiation of sperm motility after mating in the rat and hamster. J. Androl. https://doi.org/10.1002/j.1939-4640.1992.tb03341.x.

Caillard, A., Sadoune, M., Cescau, A., Meddour, M., Gandon, M., Polidano, E., Delcayre, C., DaSilva, K., Manivet, P., Gomez, A.M., et al. (2018). QSOX1, a novel actor of cardiac protection upon acute stress in mice. J. Mol. Cell. Cardiol. https://doi.org/10.1016/j.yjmcc.2018.04.014.

Chakravarthi, S., Jessop, C.E., Willer, M., Stirling, C.J., and Bulleid, N.J. (2007). Intracellular catalysis of disulfide bond formation by the human sulfhydryl oxidase. Qsox. Biochem. J. https://doi.org/10.1042/BJ20061510.

Cooper, T.G., Noonan, E., vonEckardstein, S., Auger, J., Baker, H.W., Behre, H.M., Haugen, T.B., Kruger, T., Wang, C., Mbizvo, M.T., and Vogelsong, K.M. (2010). World Health Organization reference values for human semen characteristics. Hum. Reprod. Updat *16*, 231–245. https://doi.org/10.1093/humupd/dmp048.

Cooper, T.G., Weydert, S., Yeung, C.H., Künzl, C., and Sachser, N. (2000). Maturation of epididymal spermatozoa in the nondomesticated Guinea pigs Cavia aperea and Galea musteloides. J. Androl. https://doi.org/10.1002/j.1939-4640.2000.tb03285.x.

Dohle, G.R., Smit, M., and Weber, R.F.A. (2003). Androgens and male fertility. World J. Urol. https://doi.org/10.1007/s00345-003-0365-9.

Fifield, A.L., Hanavan, P.D., Faigel, D.O., Sergienko, E., Bobkov, A., Meurice, N., Petit, J.L., Polito, A., Caulfield, T.R., Castle, E.P., et al. (2020). Molecular inhibitor of QSOX1 suppresses tumor growth in vivo. Mol. Cancer Ther. https://doi.org/10.1158/1535-7163.MCT-19-0233.

Fisher, H.S., and Hoekstra, H.E. (2010). Competition drives cooperation among closely related sperm of deer mice. Nature. https://doi.org/10.1038/nature08736.

Fornes, M.W., and Burgos, M.H. (1994). Epididymal glycoprotein involved in rat sperm association. Mol. Reprod. Dev. https://doi.org/10.1002/mrd.1080380108.

Gadella, B.M. (2017). Reproductive tract modifications of the boar sperm surface. Mol. Reprod. Dev. https://doi.org/10.1002/mrd.22821.

Gómez Montoto, L., Magaña, C., Tourmente, M., Martín-Coello, J., Crespo, C., Luque-Larena, J.J., Gomendio, M., and Roldan, E.R.S. (2011). Sperm competition, sperm numbers and sperm quality in muroid rodents. PLoS One. https://doi.org/10.1371/journal.pone.0018173.

Grossman, I., Alon, A., Ilani, T., and Fass, D. (2013). An inhibitory antibody blocks the first step in the dithiol/disulfide relay mechanism of the enzyme QSOX1. J. Mol. Biol. https://doi.org/10.1016/j.jmb.2013.07.011.

Katila, T. (2012). Post-mating inflammatory responses of the uterus. Reprod. Domest. Anim. https://doi.org/10.1111/j.1439-0531.2012.02120.x.

Kawano, N., and Yoshida, M. (2007). Semen-coagulating protein, SVS2, in mouse seminal plasma controls sperm Fertility1. Biol. Reprod. *76*, 353–361. https://doi.org/10.1095/biolreprod.106.056887.

Knutsvik, G., Collett, K., Arnes, J., Akslen, L.A., and Stefansson, I.M. (2016). QSOX1 expression is associated with aggressive tumor features and reduced survival in breast carcinomas. Mod. Pathol. https://doi.org/10.1038/modpathol.2016.148.

Kodali, V.K., and Thorpe, C. (2010). Oxidative protein folding and the quiescin-sulfhydryl oxidase family of flavoproteins. Antioxid. Redox Signal. https://doi.org/10.1089/ars.2010.3098.

Kuo, Y.W., Joshi, R., Wang, T.E., Chang, H.W., Li, S.H., Hsiao, C.N., and Tsai, P.S.J. (2017). Identification, characterization and purification of porcine Quiescin Q6-Sulfydryl Oxidase 2 protein.

BMC Vet. Res. https://doi.org/10.1186/s12917-017-1125-1.

Kuo, Y.W., Li, S.H., Maeda, K.I., Gadella, B.M., and Tsai, P.S.J. (2016). Roles of the reproductive tract in modifications of the sperm membrane surface. J. Reprod. Dev. https://doi.org/10.1262/jrd.2016-028.

Lake, D.F., and Faigel, D.O. (2014). The emerging role of qsox1 in cancer. Antioxid. Redox Signal. https://doi.org/10.1089/ars.2013.5572.

Li, S.-H., Lee, R.K.-K., Hsiao, Y.-L., and Chen, Y.-H. (2005). Demonstration of a glycoprotein derived from the Ceacam10 gene in mouse seminal vesicle Secretions1. Biol. Reprod. https://doi.org/10.1095/biolreprod.105.039651.

Li, S., and Winuthayanon, W. (2017). Collection of post-mating semen from the female reproductive tract and measurement of semen liquefaction in mice. J. Vis. Exp. https://doi.org/10.3791/56670.

Li, S.H., Hwu, Y.M., Lu, C.H., Lin, M.H., Yeh, L.Y., and Lee, R.K.K. (2018). Serine protease inhibitor SERPINE2 reversibly modulates murine sperm capacitation. Int. J. Mol. Sci. https://doi.org/10.3390/ijms19051520.

Lin, M.H., Lee, R.K., Hwu, Y.M., Lu, C.H., Chu, S.L., Chen, Y.J., Chang, W.C., and Li, S.H. (2008). SPINKL, a Kazal-type serine protease inhibitor-like protein purified from mouse seminal vesicle fluid, is able to inhibit sperm capacitation. Reproduction *136*, 559–571. https://doi.org/10.1530/REP-07-0375.

Lu, C.H., Lee, R.K., Hwu, Y.M., Chu, S.L., Chen, Y.J., Chang, W.C., Lin, S.P., and Li, S.H. (2011). SERPINE2, a serine protease inhibitor extensively expressed in adult male mouse reproductive tissues, may serve as a murine sperm decapacitation factor. Biol. Reprod. *84*, 514–525. https://doi.org/10.1095/biolreprod.110.085100.

Monclus, M.A., and Fornes, M.W. (2016). Sperm conjugation in mammal reproductive function: different names for the same phenomenon? Mol. Reprod. Dev. https://doi.org/10.1002/mrd.22636.

Ostrowski, M.C., and Kistler, W.S. (1980). Properties of a flavoprotein sulfhydryl oxidase from rat seminal vesicle secretion. Biochemistry. https://doi.org/10.1021/bi00553a016.

Ostrowski, M.C., Kistler, M.K., and Kistler, W.S. (1979a). Purification and cell-free synthesis of a major protein from rat seminal vesicle secretion. A potential marker for androgen action. J. Biol. Chem. https://doi.org/10.1016/s0021-9258(17)37929-2.

Ostrowski, M.C., Kistler, W.S., and Williams-Ashman, H.G. (1979b). A flavoprotein responsible for the intense sulfhydryl oxidase activity of rat seminal vesicle secretion. Biochem. Biophys. Res. Commun. https://doi.org/10.1016/0006-291X(79)91662-0.

Ou, C., Lee, R.K., Lin, M., Lu, C., Yang, T., Yeh, L., Tsai, P.J., and Li, S. (2021). A mouse seminal vesicle-secreted lysozyme c-like protein modulates sperm capacitation. J. Cell. Biochem. https://doi.org/10.1002/jcb.29894.

Phillips, D.M., and Bedford, J.M. (1987). Sperm-sperm associations in the loris epididymis. Gamete Res. https://doi.org/10.1002/mrd.1120180104.

Portes, K.F., Ikegami, C.M., Getz, J., Martins, A.P., DeNoronha, L., Zischler, L.F., Klassen, G., Camargo, A.A., Zanata, S.M., Bevilacqua, E., and Nakao, L.S. (2008). Tissue distribution of quiescin Q6/sulfhydryl oxidase (QSOX) in developing mouse. J. Mol. Histol. https://doi.org/10.1007/s10735-007-9156-8.

Robaire, B., and Hamzeh, M. (2011). Androgen action in the epididymis. J. Androl. https://doi.org/10.2164/jandrol.111.014266.

Robertson, S.A. (2007). Seminal fluid signaling in the female reproductive tract: lessons from rodents and pigs. J. Anim. Sci. https://doi.org/10.2527/jas.2006-578.

Rudolf, J., Pringle, M.A., and Bulleid, N.J. (2013). Proteolytic processing of QSOX1A ensures efficient secretion of a potent disulfide catalyst. Biochem. J. https://doi.org/10.1042/BJ20130360.

Sobral, A.C.L., Neto, V.M., Traiano, G., Percicote, A.P., Gugelmin, E.S., deSouza, C.M., Nakao, L., Torres, L.F.B., and deNoronha, L. (2015). Immunohistochemical expression of sulfhydryl oxidase (QSOX1) in pediatric medulloblastomas. Diagn. Pathol. https://doi.org/10.1186/s13000-015-0268-2.

Suarez, S.S. (2016). Mammalian sperm interactions with the female reproductive tract. Cell Tissue Res. https://doi.org/10.1007/s00441-015-2244-2.

Suarez, S.S., and Pacey, A.A. (2006). Sperm transport in the female reproductive tract. Hum. Reprod. Update. https://doi.org/10.1093/humupd/dmi047.

Sung, H.J., Ahn, J.M., Yoon, Y.H., Na, S.S., Choi, Y.J., Kim, Y.I., Lee, S.Y., Lee, E.B., Cho, S., and Cho, J.Y. (2018). Quiescin sulfhydryl oxidase 1 (QSOX1) secreted by lung cancer cells promotes cancer metastasis. Int. J. Mol. Sci. https://doi.org/10.3390/ijms19103213.

Taggart, D.A., Johnson, J.L., O'Brien, H.P., and Moore, H.D.M. (1993). Why do spermatozoa of American marsupials form pairs? A clue from the analysis of sperm-pairing in the epididymis of the grey short-tailed opossum, Monodelphis domestica. Anat. Rec. https://doi.org/10.1002/ar.1092360307.

Takeshima, T., Usui, K., Mori, K., Asai, T., Yasuda, K., Kuroda, S., and Yumura, Y. (2021). Oxidative stress and male infertility. Reprod. Med. Biol. https://doi.org/10.1002/rmb2.12353.

Tourmente, M., Gomendio, M., and Roldan, E.R.S. (2011). Sperm competition and the evolution of sperm design in mammals. BMC Evol. Biol. https://doi.org/10.1186/1471-2148-11-12.

Tseng, H.C., Lee, R.K., Hwu, Y.M., Lu, C.H., Lin, M.H., and Li, S.H. (2013). Mechanisms underlying the inhibition of murine sperm capacitation by the seminal protein, SPINKL. J. Cell Biochem. *114*, 888–898. https://doi.org/10.1002/jcb.24428.

Turner, T.T., Ewing, L.L., Jones, C.E., Howards, S.S., and Zegeye, B. (1985). Androgens in various fluid compartments of the rat testis and epididymis after hypophysectomy and gonadotropin supplementation. J. Androl. https://doi.org/10.1002/j.1939-4640.1985.tb03292.x.

Tury, A., Mairet-Coello, G., Esnard-Fève, A., Benayoun, B., Risold, P.Y., Griffond, B., and Fellmann, D. (2006). Cell-specific localization of the sulphydryl oxidase QSOX in rat peripheral tissues. Cell Tissue Res. https://doi.org/10.1007/s00441-005-0043-x.

Wang, T.E., Li, S.H., Minabe, S., Anderson, A.L., Dun, M.D., Maeda, K.I., Matsuda, F., Chang, H.W., Nixon, B., and Tsai, P.S.J. (2018). Mouse quiescin sulfhydryl oxidases exhibit distinct epididymal luminal distribution with segment-specific sperm surface associations. Biol. Reprod. https://doi.org/10.1093/biolre/ioy125.

STAR★METHODS

KEY RESOURCES TABLE

REAGENT or RESOURCE	SOURCE	IDENTIFIER
Antibodies		
Rabbit polyclonal anti-QSOX1	This paper	N/A
Mouse monoclonal anti-β-actin	Cell Signaling Technology	#3700; RRID:AB_2242334
Rabbit polyclonal anti-EEF2	Abcam	#ab40812; RRID:AB_732082
Goat anti-rabbit IgG H&L (Alexa Fluor® 594)	Abcam	# ab150080; RRID:AB_2650602
Goat anti-rabbit IgG (H+L), Fluorescein	Vector Laboratories	# FI-1000-; RRID:AB_2336197
Mouse monoclonal anti Phosphotyrosine Antibody, clone 4G10	Millipore	# 05-321; RRID:AB_309678
Biological samples		
Human semen	This paper	N/A
Adult mouse tissues	This paper	N/A
Chemicals, peptides, and recombinant proteins		
THIOLYTE monobromobimane	Merck	#596150
Calcium Ionophore A23187	Sigma-Aldrich	#C7522
Lectin from Arachis hypogea (peanut)	Sigma-Aldrich	#L7381
PureSperm 40/80	Nidacon International AB	#PSK-020
Bovine serum albumin	Sigma-Aldrich	#A0281
QSOX1 protein purified from mouse seminal vesicle secretion	This paper	N/A
DEAE Sephacel	GE Healthcare	#17-0500-01
ProLong Gold Antifade Mountant	Thermo Fisher Scientific	# P36930
Critical commercial assays		
CellROX Green Reagent	Thermo Fisher Scientific	#C10444
MitoTracker Red CM-H_2Xros	Thermo Fisher Scientific	Cat#M7513
LIVE/DEAD Sperm Viability Kit	Thermo Fisher Scientific	Cat#L7011
Dead Cell Apoptosis Kit with Annexin V Alexa Fluor™ 488 & Propidium Iodide (PI)	Thermo Fisher Scientific	Cat#V13241
OxiSelect Total Antioxidant Capacity (TAC) Assay	Cell Biolabs	Cat#STA-360
Experimental models: Organisms/strains		
Mouse: CD-1	BioLASCO Taiwan	N/A
Oligonucleotides		
The forward primer for the preparation of the *Qsox1* probe used in Northern blotting: 5′-ctggcttcccgactgtgaggtttt-3′	This paper	N/A
The reverse primer for the preparation of the *Qsox1* probe used in Northern blotting: 5′-ggtagcccccgaagataggatgta-3′	This paper	N/A
The forward primer for the preparation of the *Gapdh* probe used in Northern blotting: 5′-cggcaaattcaacggcacagt-3′	This paper	N/A
The reverse primer for the preparation of the *Gapdh* probe used in Northern blotting: 5′-tgggggtaggaacacggaagg-3′	This paper	N/A

(*Continued on next page*)

Continued

REAGENT or RESOURCE	SOURCE	IDENTIFIER
Software and algorithms		
ImageJ	NIH	https://imagej.nih.gov/ij/
Prism 6	GraphPad	https://www.graphpad.com/scientific-software/prism/
cellSens	Olympus	https://www.olympus-lifescience.com.cn/en/software/cellsens/
Other		
Protein-Pak SP 5PW Column	Waters	#WAT088043
Alliance Separations Module e2695	Waters	https://www.waters.com/waters/library.htm?locale=180&cid=534293&lid=134721256

RESOURCE AVAILABILITY

Lead contact

Further information and requests for resources and reagents should be directed to and will be fulfilled by the lead contact, Sheng-Hsiang Li (lsh@mmh.org.tw).

Materials availability

Further information and requests for resources and reagents should be directed to and will be fulfilled by the lead contact

Data and code availability

- All data are included in the manuscript and Supplemental information
- This paper does not report original code
- Any additional information required to reanalyze the data reported in this paper is available from the lead contact upon request

EXPERIMENTAL MODEL AND SUBJECT DETAILS

Human semen collection

Donors collected semen samples through masturbation after 2–3 days of abstinence. After liquefaction for at least 30 min, semen samples with sperm motility >40% and sperm concentration >15 million/ml met the 2010 World Health Organization criteria (Cooper et al., 2010) were included in the study. The use of human semen for research has been reviewed and approved by the Institutional Review Board of the MacKay Memorial Hospital (approval number: 17MMHIS180).

Mice

Specific pathogen-free outbred CD-1 male mice (BioLASCO Taiwan, Yilan, Taiwan) 10-12 weeks old and female New Zealand white rabbits (Animal Health Research Institute, Miaoli, Taiwan) weighing 2.0-2.5 kilograms were bred following institutional guidelines for the care and use of experimental animals. All animal experiments were approved and carried out under the regulation and permission of Institutional Animal Care and Use Committee protocols at National Taiwan University (approval numbers: NTU-103-EL-86 and NTU-104-EL-00081) and MacKay Memorial Hospital (approval number: MMH-M-S-101-14). Animals were housed under controlled lighting (cycle of 14 h light and 10 h dark) at 21–22°C and had free access to food and water.

METHOD DETAILS

Purification of mouse QSOX1c protein

Adult male mice (10–12 weeks old) were euthanized by CO_2 followed by cervical dislocation. The seminal vesicles of 50 mice were dissected to free them from the adjacent coagulating glands. The secretions were squeezed directly into 50 ml of ice-cold 10 mM Tris-HCl in the presence of 1 mM phenylmethylsulfonyl

fluoride at pH 8.0. After centrifugation at 10,000 × *g* for 15 min, the supernatant was resolved to four fractions by ion-exchange chromatography on a DEAE-Sephacel column (12 × 2.6 cm) (Figure S1A) as previously described (Li et al., 2005). Fraction III with a yellow color was further resolved into peaks a-e (Figure S1B) by ion-exchange HPLC on a sulfopropyl column (7.5 cm × 7.5 mm) with linear gradients (Li et al., 2005). A total of 150 mice were divided into three batches for the collection of SVS and purification of QSOX1c.

Mass spectrometry analysis

The fraction from HPLC peak e was resolved on the sodium dodecyl sulfate-polyacrylamide gel electrophoresis (SDS-PAGE) (Figure S1C), distinct protein band (indicated with red arrowhead) from Pe lane was excised, washed in a solution containing acetonitrile and 100 mM NH_4HCO_3 (1:1, v/v), and subjected to in-gel digestion with trypsin overnight at 37°C. The digested peptides were extracted with a solution of 50% (v/v) acetonitrile and 1% (v/v) formic acid and lyophilized. To carry out mass spectrometric analyses, the peptide solution was redissolved in 30 μl 0.1% (v/v) formic acid, mixed with an equal volume of the matrix solution [1% α-cyano-4-hydroxycinnamic acid, 50% (v/v) acetonitrile, and 0.1% (v/v) trifluoroacetic acid], allowed to air-dry, and analyzed with a Voyager Elite mass spectrometer (PerSeptive Biosystems, Framingham, MA). Peptide sequences were identified by Mascot software (Matrix Science, London, UK) analysis. Automated Edman degradation was conducted to determine the N-terminal amino acid sequence using the Applied Biosystems LC 494 Procise Protein Sequencing (Foster City, CA).

Production of anti-QSOX1c antisera

Antisera were produced using New Zealand white rabbit. Purified mouse QSOX1c protein in normal saline (0.5 mg/ml) was emulsified with Freund's complete adjuvant (1:1, v/v). In total, 2 ml of the mixture was subcutaneously injected in multiple sites in individual rabbits (n = 2). Rabbits were boosted twice every 3 weeks with the mixture of the purified protein and Freund's incomplete adjuvant. Antisera were collected 10 days after the last injection.

Western blotting

Mouse reproductive tissues were obtained and homogenized with an ice-cold homogenization buffer as previously described (Kuo et al., 2017; Wang et al., 2018). An equivalent amount of protein extract (50 μg) was resuspended with an appropriate volume of lithium dodecyl sulfate loading buffer (Invitrogen) in the presence of reducing agent (50 mM dithiothreitol); samples were heated in a 100°C dry bath for 10 min and air-cooled to room temperature (RT) before loading on gels. Bio-Rad Mini-PROTEIN electrophoresis system (Bio-Rad Laboratories Ltd., Hertfordshire, UK) was used, and standard manufacturer's protocols were followed. Proteins were separated by 10% SDS-PAGE (gradient T-Pro EZ Gel Solution, T-Pro Biotechnology, NTC, TW) and wet-blotted onto a polyvinylidene fluoride membrane (Immobilon-P, Millipore, Billerica, MA). After blocking with blocking buffer [5 mM Tris-HCl, 250 mM sucrose, pH 7.4, and 0.05% (v/v) Tween-20 (TBST), supplemented with 5% milk powder] at RT for 1 h, blots were incubated with anti-QSOX1c antiserum (1:5000 dilution), anti-β-actin (1:10,000), or anti-EEF2 (1:50,000) at RT for 1 h. After three times of washing in TBST, a secondary antibody was subsequently added, and blots were incubated at RT for 1 h. After rinsing with TBST, a specific protein signal was visualized using chemiluminescence (Merck, Ltd., TW) and detected under ChemiDoc MP (Bio-Rad Laboratories, Hercules, California). The relative intensity of each band was determined using ImageJ software (NIH; https://imagej.nih.gov/ij/).

Animal castration and hormone challenge model

To evaluate testosterone's effects on QSOX1 expression in the male reproductive tract, we performed a modified castration process to remove only the testes in 12-week-old adult males (n = 15) and left the epididymides, seminal vesicles, and vas deferens in the animal. The mouse was anesthetized with 1-3% isoflurane in oxygen. The core body temperature was maintained between 36°C to 38°C by a heating pad. The vital signs, respiratory pattern, blood pressure, electrocardiography, and end-tidal CO_2 were monitored continuously throughout the surgery. After removal of hair and sanitize with iodine, testes from both sides of the scrotum were exposed. Removal of testis was carefully performed by separation of the testis from the epididymis; after blood vessels and the efferent duct were ligated, testis was removed. Mice were allowed to recover for 14 days before administration of testosterone propionate (Sigma-Aldrich) dissolved in corn oil (5 mg/kg body weight) for 8 consecutive days (n = 6, castration + testosterone group); the other 6

castrated animals received corn oil only (vehicle control, n = 6, castration + corn oil group), three animals were served as surgical control that the same surgical procedures were performed without removal of the testes.

Northern blotting

Total RNA was extracted using a TRIzol reagent (Thermo Fisher Scientific). Polymerase chain reaction-amplified fragments of *Qsox1* cDNA (454 bp) or glyceraldehyde-3-phosphate dehydrogenase (*Gapd*) cDNA (557 bp) were used as the templates to prepare the ^{32}P-labeled cDNA probe using a random-priming kit (Sigma-Aldrich). RNA samples (5 μg) were subjected to 1.0% (w/v) agarose-formaldehyde gel electrophoresis, blotted onto nylon membranes by capillary transfer, and hybridized with the probe following a previously published paper (Li et al., 2005). In brief, blotted membranes were first hybridized with *Qsox1* probes overnight at 65°C, and then the free probes were washed out. Messenger RNA signals on the membranes were examined using a Fuji phosphorimager (Fuji Laboratories, Japan). Then, membranes were hybridized with the *Gapd* probes in the same way after removing the *Qsox1* probes. Thus, hybridization with the *Qsox1* and *Gapd* probes was performed on the same membranes.

Immunofluorescence staining on tissue sections

Indirect immunofluorescence staining was performed as previously described (Wang et al., 2018). Paraffin-embedded tissue sections were deparaffinized in 100% xylene and rehydrated with 100%–80% ethanol. Antigen retrieval was carried out by heating tissue sections in 10 mM citrate buffer (pH 8.0) using a regular microwave at 95°C and 104°C for 5 min at each temperature. After blocking with 1% bovine serum albumin (BSA) for 1 h at RT, tissue sections were further permeabilized with 0.1% Triton-X 100 at RT for 5 min. Anti-QSOX1c antiserum was used at a dilution of 1:5000 and incubated overnight at 4°C. Sections were then incubated with goat anti-rabbit Alexa-594 (1:150 diluted) for 1.5 h at RT. Nuclei were stained with 4′, 6-diamidino-2-phenylindole (DAPI) (Vectashield H-1200, Vector Laboratories, CA), and slides were sealed with nail polish. As for negative controls, each immunoreaction was accompanied by a reaction omitting the primary antibody. All samples were evaluated using Olympus IX83 epifluorescence microscopy and analyzed with either ImageJ or CellSens software (Tokyo, JP). Background subtraction was performed identically for all images in the same experiment.

Sperm capacitation and acrosome reaction

To minimize individual variations in sperm concentration and sperm quality, sperm cells from 2-3 male mice were mixed and used for each sperm assay. Mouse cauda epididymal sperm cells were obtained as previously described (Wang et al., 2018). In brief, after mice were euthanized with CO_2, the caudal epididymis and vas deferens were immediately removed. Sperm cells were collected from cauda epididymis to Biggers, Whitten, and Whittingham (BWW) medium containing NaCl (91.5 mM), KCl (4.6 mM), KH_2PO_4 (1.2 mM), $MgSO_4$ (1.2 mM), glucose (5.6 mM), pyruvic acid (0.27 mM), sodium lactate (44 mM), $CaCl_2$ (1.7 mM), and HEPES (20 mM). The medium was adjusted to pH 7.4 and sterilized by filtration through a 0.22-μm membrane filter (Millipore, SA). After sperm cells swim out from epididymal tubules on a thermo-controlled (37°C) working stage (Tokai HIT, Tokyo, Japan), the sperm suspension was collected and incubated at 37°C for a further 15 min to allow the motile sperm to swim upward. We then collected the upper half layer of the sperm suspension and adjusted the sperm concentration to 10^6 sperm/ml for further assays.

Epididymal spermatozoa were pre-incubated with or without QSOX1c (0.3, 0.6, or 0.9 mg/mL) in BWW medium for 15 min and then capacitated with or without BSA (3 mg/ml) and $NaHCO_3$ (25 mM), at 37°C in humidified air with 5% (v/v) CO_2 for 90 min. Sperm proteins were then extracted, resolved on an 8% SDS-PAGE gel, electrotransferred onto a nitrocellulose membrane, and Western blotting using an anti-phosphotyrosine monoclonal antibody (1:5000 dilution, clone 4G10, Millipore, Temecula, CA) following the previously published method (Ou et al., 2021).

For the induction of acrosome reaction, the capacitated sperm were treated with or without 10 μM A23187 in 0.1% (v/v) dimethyl sulfoxide at 37°C for 30 min. Sperm were then washed and smeared onto a slide following the method mentioned above (Ou et al., 2021). The acrosomal status was revealed by staining with 5 μg/mL of PNA-FITC (Sigma-Aldrich) for 10 min in the dark. After counterstaining with Hoechst 33258 (5 μg/ml) for 30 s, the slide was mounted with Prolong Gold antifade medium (Invitrogen Molecular

Probes) and examined with a fluorescence microscope (BX 53, Olympus). A random sample of 200 sperm cells per group was evaluated.

Sperm oxidative status assays

To evaluate mitochondria function and oxidative status of sperm cells, commercially available OxiSelect assay for total antioxidant capacity measurement (Cell Biolabs, Inc., CA), MitoTracker Red CM-H_2XRos for mitochondria oxidation status, and CellROX green reagent for the detection of oxidative stress in live sperm cells were used respectively. For TAC assay, sperm lysates from each condition were added into a 96-well microtiter plate and mixed with a reaction buffer. Copper ion reagent was added into each well and incubated for the required time on a shaker to initiate the reaction. Stop solution was subsequently added into the well before reading optic density values at 490 nm. For mitochondria status evaluation, after treatments, sperm cells were rinsed with BWW medium before the incubation of 500 nM MitoTracker Red CM-H_2XRos for 30 min at 37°C. After staining, cells were rinsed and fixed with 4% paraformaldehyde, and cell nuclei were stained with DAPI. More than 200 sperm cells from each group were manually counted, and mitochondria health was evaluated and expressed as the % of cells with strong intensity for MitoTracker Red CM-H_2XRos.

In vitro sperm aggregation assay

We prepared fresh mouse epididymal sperm (~10^6 cells/ml) as described above. For in vitro human sperm analysis, motile sperm was isolated using PureSperm (Nidacon International AB, Mölndal, Sweden) discontinuous density gradient centrifugation. In short, 1 ml liquefied semen was layered on top of a PureSperm gradient solution prepared by stacking 1 ml PureSperm40 on 1 ml PureSperm80 solution. After centrifuging at 300 × g for 20 min, the upper supernatant was removed except the lowest 0.5 ml and resuspended in 5 ml BWW medium. After washing through BWW again, we collected the lowest 0.1 ml and adjusted the sperm concentration to 10^6 sperm/ml for further assays.

Before adding the sperm suspension, freshly prepared control media (BWW) and tested group (BWW +0.15 mg/ml of QSOX1c) were kept in a 5% CO_2, 37°C incubator. Sperm aggregation assay was performed in 96-well plates with a total volume of 100 µl/well; subsequent observations, images, and videos were taken at 10, 30, 60, and 90 min after incubation under an Olympus IX83 inverted microscope equipped with a live cell system (Tokai Hit, Shizuoka, Japan). To quantify the amount of sperm agglutination, we defined a "sperm aggregation index" as the area of sperm aggregates within the circle (marked in green using Olympus CellSens software) divided by the total area of the marked circle (indicated by red) (Figure S4A). To evaluate QSOX1c ability on sperm aggregation, we also defined the "QSOX1c aggregation index" as the number of events counted in the region of interest (ROI, green) divided by total events within the area of examination (red) (Figure S4B).

To assess the cellular status of agglutination sperm, after 30 min of sperm aggregation assay, the solution was incubated with the following reagents at 37°C for another 20 min: (1) CellROX (5 µM) + propidium iodide (PI, 5 µg/ml); (2) mBBr (20 µM) + PI (5 µg/ml); (3) Annexin V Alexa Fluor 488 (5 µM) + PI (5 µg/ml). The solution was centrifuged at 200 × *g* for 5 min to remove free reagents. The sperm pellet was resuspended in BWW medium, smeared on a slide, covered with a coverslip, and then photographed using an epifluorescence microscope (IX73, Olympus) equipped with a CCD camera (DP73, Olympus).

In vivo sperm aggregation assay

For in vivo mouse sperm preparation, female mice (3 weeks old) were superovulated with 5 IU of pregnant mare serum gonadotropin (Sigma-Aldrich) and 48 h later with 5 IU of human chorionic gonadotropin (Sigma-Aldrich). They then were mated with mature male mice (12 weeks old). When the vaginal plug was formed, the female mice were sacrificed. Clamped the two uterine horns, cut off the uterus, and dripped and squeezed the semen into a vial containing 500 µl BWW medium (prewarmed at 37°C). To prevent more white blood cells from infiltrating and collect live sperm and sperm agglomerates, we only collected semen within one hour after mating. Gently tapped the vial with fingers to evenly mix the semen and medium.

To examine whether there are agglutinated sperm in the semen, we briefly washed the semen by mixing 1 ml liquefied human semen with 3 ml BWW medium and centrifuging at 300 × *g* for 5 min. The sperm pellet

was resuspended in 3 ml BWW medium, centrifuged again, and adjusted the sperm concentration to approximately 10^6 sperm cells/ml for the following analysis.

To assess the cellular status of agglutination sperm, we incubated mouse semen solution or the washed human semen with the following reagents in 200 μl BWW medium for 20 min at 37°C: (1) CellROX (5 μM) + PI (5 μg/ml); (2) mBBr (20 μM) + PI (5 μg/ml); (3) Annexin V Alexa Fluor 488 (5 μM) + PI (5 μg/ml). The solution was centrifuged at 200 × *g* for 5 min to remove the free reagents. The sperm pellet was resuspended in BWW medium, smeared on a slide, covered with a coverslip, and photographed using an epifluorescence microscope (IX73, Olympus) equipped with a CCD camera (DP73, Olympus).

To assess whether QSOX1 is present in the agglutination sperm, we smeared the semen on the slide to air-dry and fixed it with 10% buffered neutral formalin for 20 min. After washing with PBS twice for 5 min, the slide was treated with PBS containing 10% normal goat serum (blocking solution) for 1 h at 37°C. The slides were then incubated with the anti-QSOX1c antiserum (1:100) in blocking solution at 37°C for 1 h, washed thrice for 5 min with PBS, and developed for 1 h with FITC-conjugated goat anti-rabbit IgG (Vector Laboratories) diluted 1:100 in blocking solution. After washing as above, slides were counterstained with 5 μg/ml Hoechst 33258, mounted in 100 μl of ProLong Gold antifade medium (Molecular Probes, Eugene, OR), and photographed using an epifluorescence microscope (BX 53, Olympus, Tokyo, Japan) equipped with a CCD camera (DP71, Olympus).

QUANTIFICATION AND STATISTICAL ANALYSIS

All values are presented as mean ± standard deviation (SD). One-way analysis of variance (ANOVA) with Tukey's multiple comparisons test or two-tailed Student's *t*-test was used to evaluate statistical differences between groups using GraphPad Prism version 6 (GraphPad Software). Differences were considered statistically significant at $p < 0.05$.